Path-Loss and Time Dispersion Parameters for Indoor UWB Propagation

A. Muqaibel, A. Safaai-Jazi, A. Attiya, B. Woerner, and S. Riad, *Fellow, IEEE*

Abstract— The propagation of ultra wideband (UWB) signals in indoor environments is an important issue with significant impacts on the future direction and scope of the UWB technology and its applications. The objective of this work is to obtain a better assessment of the potentials of UWB indoor communications by characterizing the UWB indoor communication channels. Channel characterization refers to extracting the channel parameters from measured data. An indoor UWB measurement campaign is undertaken. Time-domain indoor propagation measurements using pulses with less than 100 ps width are carried out. Typical indoor scenarios, including line-of-sight (LOS), non-line-of-sight (NLOS), room-to-room, within-the-room, and hallways, are considered. Results for indoor propagation measurements are presented for local power delay profiles (local PDP) and small-scale averaged power delay profiles (SSA-PDP). Site-specific trends and general observations are discussed. The results for path-loss exponent and time dispersion parameters are presented.

Index Terms— Ultra-wide bandwidth, path loss, in building propagation, propagation channel, impulse radio, indoor radio communication.

I. INTRODUCTION

ULTRA WIDEBAND (UWB), wireless communication has been the subject of extensive research in recent years due to its potential applications and unique capabilities. However, many important aspects of UWB-based communication systems have not yet been thoroughly examined. The propagation of UWB signals in indoor environments is one of the important issues with significant impacts on the future direction, scope, and generally the extent of the success of UWB technology. Researchers are nowadays devoting considerable efforts and resources to develop robust channel models that allow for reliable and accurate ultra-wideband performance simulation.

In the past two decades, significant research work has been devoted to narrowband indoor channel characterization. Of particular interest are investigations carried out by Saleh

Ali Hussein Muqaibel is with King Fahd University of Petroleum and Minerals, P. O. Box 1734, Dhahran, 31261, Saudi Arabia (e-mail: muqaibel@kfupm.edu.sa).

Ahmad Safaai-Jazi and Sedki Riad are with the Department of Electrical and Computer Engineering, Virginia Tech, Blacksburg, VA 24060 USA (e-mail: ajazi@vt.edu; sriad@vt.edu).

Ahmed M. Attiya is with the University of Mississippi, Room 101, Engineering Science Building, University, MS 38677 USA (email: attiya@olemiss.edu).

Brian Woerner is with West Virginia University, 825 Engineering Sciences Building, Morgantown, WV 26506 USA (email: brian.woerner@mail.wvu.edu).

and Valenzuela [1], Hashemi [2], [3], Anderson et al. [4], Durgin and Rappaport [5], and Rappaport [6], [7], [8], whose primary objective has been to develop channel models that describe the system performance adequately. Successful channel characterizations require extensive and accurate propagation measurements. At present, the amount of available UWB measurement data is very limited and more are needed to support a comprehensive channel modeling study. The issue becomes more complicated due to the fact that UWB pulse measurements are antenna dependent. The spectrum and the shape of the pulse also affect the measurements.

The analysis of indoor communication systems based on simulation of the entire transmission link using statistical methods is most useful in assessing the system performance [2]. This approach, however, requires extensive propagation measurements. Some research work on both deterministic [9] and statistical modeling [10], [11] has been reported. More recently, Cassioli et al. [12] presented simulation results for UWB indoor communications, while Chalillou et al. [13] discussed the main structure of a general simulator for UWB communication systems. However, there still remain many unresolved issues and hence the need for more UWB propagation measurements. Different measurement conditions, insufficient measurement data, and the effect of different excitation pulses are among the priority issues that demand additional measurements in order to formulate robust models before designing simulators.

Recently, Scholtz and Win conducted a UWB time-domain measurement campaign [14]. The results of these measurements were later used to develop further models [11], [15], but no information on the pulse shape and the characteristics of the antennas used in their measurements are explicitly provided. Only in a separate study it is mentioned that a diamond dipole antenna has been used [16]. In order to achieve a more realistic characterization of UWB channels, Withington et al. [17] and Dickson and Jett [18] used modulated and time dithered pulses to emulate real communication environments. However, if the transfer function or the impulse response of the channel is known, it will be a relatively straightforward task to study the effects of time dithering or any other techniques through simulation.

Another approach for UWB channel characterization is to perform propagation measurements in the frequency domain and convert the results to the time domain by means of inverse Fourier transform. The advantage of this approach is that the sensitivity of the equipment used, particularly the vector network analyzer, is much higher than that used for time-domain measurements such as sampling oscilloscope. The

chief disadvantage of frequency-domain measurements is that long high-quality RF cables are required for connecting the network analyzer to both receiving and transmitting antennas [19]. Furthermore, double shielding of these cables is often required in order to prevent coupling of radiated signals through the cable from the air to the receiver. These cables represent a major limitation for long distance measurements. On the other hand, in direct time-domain measurements, it is only required to use a cable for carrying the triggering signal from the source at the transmitting side to the sampling oscilloscope at the receiving end. The bandwidth of the triggering signal is usually much less than the bandwidth of the pulse. Thus, long cables with moderate attenuation and bandwidth are adequate for triggering purposes, making time-domain measurements of UWB signals for longer distances between the source and the observation point much easier.

A number of researchers have studied UWB channel propagation using frequency-domain measurements, including Ghassemmzadeh et al. [19], Prettie et al. [20], Keignart and Daniele [21], Kunisch and Pamp [22], Street et al. [23], and Hovinen et al. [24]. Only Ghassemmzadeh et al. [19] used substantially long cables, up to 45 m, while most others who have described their measurement setups have used cables of up to nearly 10 m. They have also used different signal bandwidths in their measurements. The time-domain resolution and the time delay that can be obtained from frequency-domain measurements depend on the minimum and the maximum frequencies in a given bandwidth and the number of frequency points at which measurements are taken. Channel models based on frequency-domain measurements and in specific frequency bands are suitable for interference studies, but cannot be directly used for UWB channel characterization [25].

The objective of this paper is to present time-domain measurements and characterization of ultra wideband (UWB) propagation in indoor environments and to detail the experimental procedures and measurement setup used to collect data. First, experimental procedures and locations where the measurements were carried out are described in detail. Then, post-processing of the acquired data is explained. Finally, the results pertaining to the signal quality, small-scale effects, large-scale path-loss exponents, and time dispersion parameters are discussed. Some site-specific trends and observations are described and channel performances for two types of directive and omni-directional antennas are compared.

II. MEASUREMENT PROCEDURE AND LOCATIONS

A. Measurement Procedure and Setup

Time-domain measurements were performed using a sampling oscilloscope as receiver and a Gaussian-like pulse generator as transmitter. Two low noise wideband amplifiers were used at the receiver side. Each amplifier has a gain of 10 dB and a 3dB-bandwidth of 15 GHz. The width of the excitation pulse is less than 100 ps. Offset calibration is carried out with a matched load before performing any measurements. The received signals were sampled at a rate of 1 sample per 10 ps. An acquisition time window of 100 ns was selected to ensure that all observable multipath components are accounted

for. This time window is consistent with the maximum excess delay of 70 ns reported by other investigators [24]. The sampling oscilloscope allows a maximum of 5K points at a time. The 5K points correspond to 50 ns time window. Two measured 50 ns time windows were cascaded to yield a 100 ns acquisition time. A total of about 400 profiles were collected. The spatial width of the used pulse in our measurements is much smaller than the one used in previously published measurements. The spatial width is small enough to make the line-of-sight path always resolvable from any other multipath component. Information about the excitation pulse allows for deconvolution and hence generalization of results for use in other communication applications in the covered frequency range [26].

In indoor environments, the time-varying part of the impulse response is typically due to human movements. By conducting measurements during low activity periods and by keeping both the transmitter and the receiver stationary, the channel can be treated as being quasi-stationary. This allows us to average 32 measurements, thus effectively canceling out the noise.

Two different sets of measurements were performed using highly directional TEM horn antennas and omni-directional biconical antennas. Both transmitter and receiver antennas were placed on plastic moving carts at an elevation of about 1.25 m above the floor. Styrofoam slabs were used to adjust the elevation without introducing significant reflections around the antennas. The TEM horn antennas were aligned for maximum boresight reception. The advantage of using TEM horn antennas is that they are ultra wideband radiators designed and optimized for time-domain impulse response measurements. TEM horn antennas emulate sectored antennas proposed for GHz bandwidth indoor applications. These antennas have narrow beamwidths and thus are highly directional. With TEM horns, fewer multipath components are received, and almost none from rear directions of the receiver. TEM horns have been used for channel characterization in the past. For example, Davis et al. [27] and Anderson et al. [4] used a TEM horn as the transmitting antenna and a TEM horn or an omnidirectional antenna as the receiving antenna for channel characterization in the 60 GHz frequency band. The extent of multipath effects due to directional antennas on measurements is highlighted in [5]. On the other hand, biconical antennas are omni-directional and are more appropriate representative of antennas to be used in mobile UWB applications. The biconical antennas used in this investigation have not been designed as impulse antennas but have very wide input-impedance bandwidth.

Two levels of measurements are performed to characterize the small-scale and the large-scale fading parameters of the channel. Initially, a 7×7 grid with 15 cm spacing between adjacent points was designed and used in the measurements. However, after observing that no small-scale fading due to phase cancellation occurs, only a 3×3 measurement grid with 45 cm spacing between adjacent points was used. The triggering signal was carried by a coaxial cable to the sampling oscilloscope. As the distance between transmitter and receiver increases the loss and dispersion in the triggering cable increase too, resulting in a higher jitter. An effort was made to use higher quality cables and minimum possible lengths for the triggering cable. A personal computer was used to store
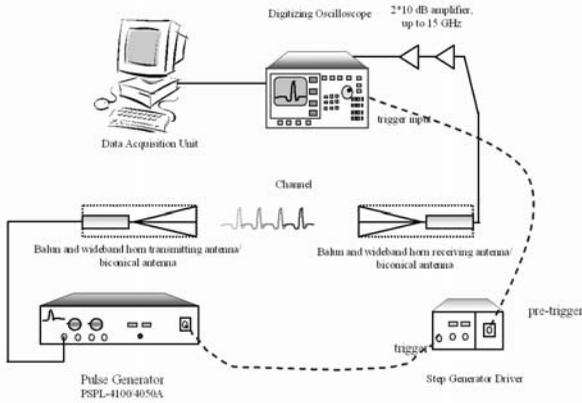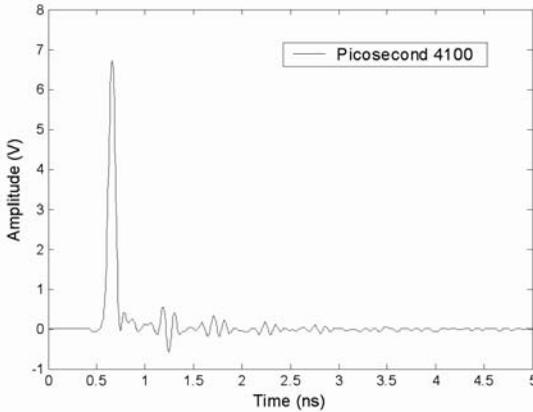
Fig. 1.   Time-domain measurement setup.

Fig. 2.   Gaussian-like output waveform of pulse generator.

and post process the data. The measurement setup is illustrated in Fig. 1 and the excitation pulse is shown in Fig. 2.

B. Description of Measurement Locations

The measurements were carried out in two buildings on Virginia Tech Campus; namely, Whittemore Hall and Durham Hall. The former building comprised mainly of offices and classrooms with most walls made of drywalls with metallic studs. Some walls at certain locations including stairwells are made of cinderblock and poured concrete. In Durham Hall, interior walls are largely made of drywalls and cinderblocks. The floor is covered with tiles in hallways and with carpet inside the rooms. An advantage of performing UWB experiments in these buildings is that they have been characterized for some narrowband measurements and site-specific ray tracing studies [4], [6], [28], [29], [30]. This allows one to compare the narrowband and the UWB channel characterization results.

In Whittemore Hall, the measurements were performed in three different floors; along the hallways on the second floor, in a narrow corridor on the fourth floor and in a conference room on the sixth floor. Figure 3(a) shows the blueprints of the second floor and the location of the performed measurements. In Durham Hall, all measurements were carried on the fourth floor. Five different transmitter locations were considered. For
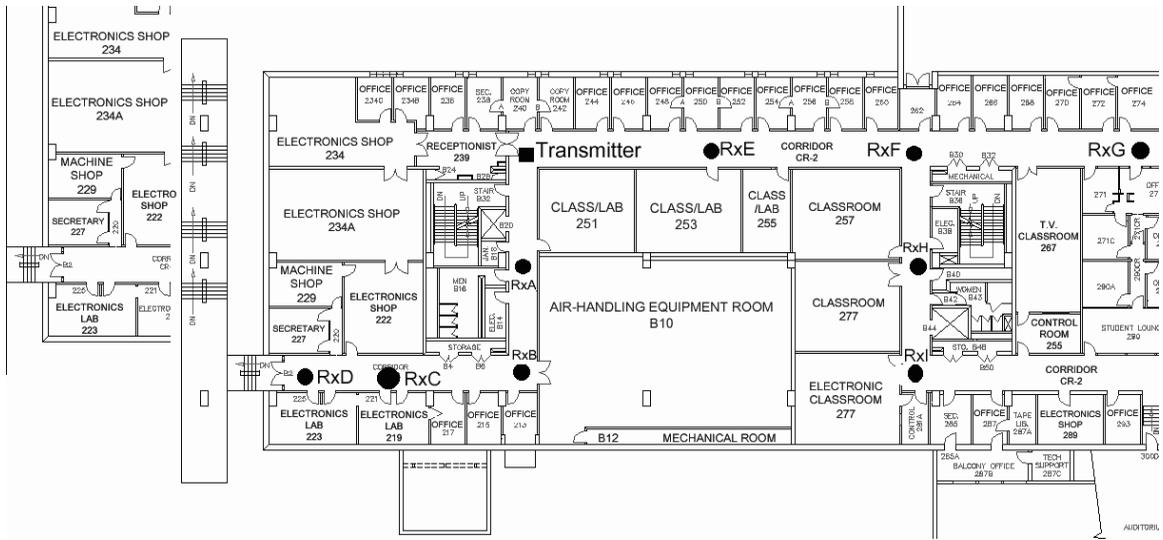
every transmitter location, measurements at different receiver locations were performed, as indicated by Tx1 through Tx5 on the blueprints in Fig. 3(b). Different scenarios are considered. Line-of-sight (LOS) and non-line-of-sight (NLOS) topographies are of particular interest. Room-to-room, within-the-room and hallways are all typical indoor measurement scenarios. Shadowing effects can also be assessed in some scenarios.

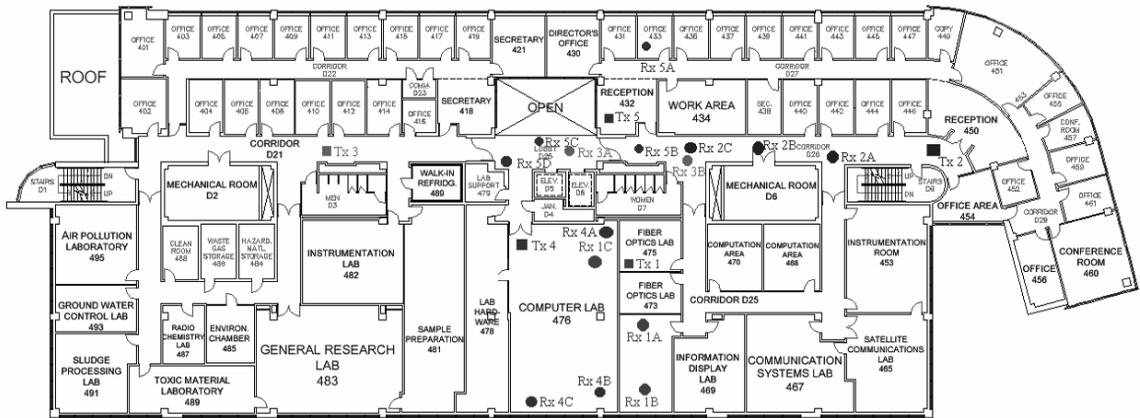### III. SIGNAL PROCESSING AND DATA ANALYSIS

A major challenge in UWB channel measurements is that the measurement bandwidth is open to any signal. When taking measurements close to utility rooms or laboratories where electromagnetic radiation level is high, there is an apparent increase in the noise floor. To reduce the interference from undesirable sources, the acquired signal profile is filtered in the time domain to remove some signals that are not part of the transmitted pulse. The 3 dB bandwidth of the bandpass filter used for interference rejection occupies a frequency range from 0.1 GHz to 12 GHz. The corner frequencies of the filter are chosen by observing the spectrum of the radiated pulse and making sure that there is no significant energy outside the filter pass band. The filtering process has three advantages. First, the noise energy is reduced by eliminating out-of-band noise resulting from over sampling. Second, any dc offset that has not been taken into account by the calibration is removed. Finally, the lower frequency signals radiated from the pulse generator's internal electronics are eliminated. It was noted that the pulse generator gives off low frequency components in the 30 MHz range that can be picked up by the biconical antenna.

Precursor and noise before the arrival of the first component are forced to zero in the processing stage. For energy calculations and large-scale path-loss analysis, a noise threshold is introduced below which all data are assumed to be zero. The threshold was set at 6 dB above the noise floor determined as the maximum level of the profile tail in the last 5 ns of the 100 ns time window.

Due to the direct impact of the used antenna on the measurements, the results from measurements with the TEM horn and biconical antennas are presented separately. At five receiver locations no signal could be clearly detected by the TEM horn antenna. At the first four locations there was no line-of-sight between the transmitter and the receiver, because the obstructed path is either through concrete walls or through multiple drywalls on metallic studs. These four locations correspond to RxC, RxD, RxH, and RxI in Fig. 3(a). The insertion loss is a function of frequency. Thick reinforced concrete walls are essentially impenetrable at high frequencies [27]. At the fifth location indicated by Rx4B in Fig. 3(b), the line-of-sight is obstructed with office cubical metallic partitions. The use of the omnidirectional antenna did not improve the measurements at those locations. The reason is that the pulse spectrum contains substantial high frequency contents. At higher frequencies, the line-of-sight component is the most significant part, since diffracted components and through-the-wall propagation are much weaker. Moreover, indoor path loss generally increases with frequency. Small-scale effects, large-

(a) Whittemore Hall (second floor only).

(b) Durham Hall (squares represent transmitter locations, circles represent receiver locations).

Fig. 3.   Blueprints of measurement locations and environments.

scale path-loss and time dispersion parameters are discussed separately in the following subsections.

A. Small-Scale Fading and Signal Quality

In narrowband communication systems, small-scale fading describes signal fluctuations due to constructive and destructive interference of the multipath components at the receiver when sub-wavelength changes are made in the receiver position [5], [8]. The concept of small-scale fading may be extended to UWB communications as the constructive and destructive interference of multipath components at the receiver due to a change in its position in the order of fraction of spatial width of the transmitted pulse.

Sample results are presented for measured delay profiles, referred to as local power delay profiles (local PDP) and for small-scale averaged power delay profiles (SSA-PDP). In SSA-PDPs, nine measurements are properly delayed and

averaged. Figure 4 illustrates how SSA-PDPs are different from the local PDPs. The first three plots are local PDPs and the last one, is the average of all 9 local measurements. When delay-and-average is used, the line-of-sight components tend to prevail and the other components spread out on the time axis such that they do not add coherently because of the high resolution of the transmitted pulse. Small-scale processing shows the capability for using a delay-and-sum beamformer to process a received array of signals from different antennas located in a very small area [31]. It is important to note that small-scale and large-scale terminologies have been used as relative measures of distances between the receiver locations compared with the wavelength. These terminologies do not fit well to our analysis because any movement tends to be large compared to the effective wavelength.

In narrow-band measurements, the spacing between the local measurements is related to the wavelength, λ. It is reported in [32] that one can cancel out small-scale effects
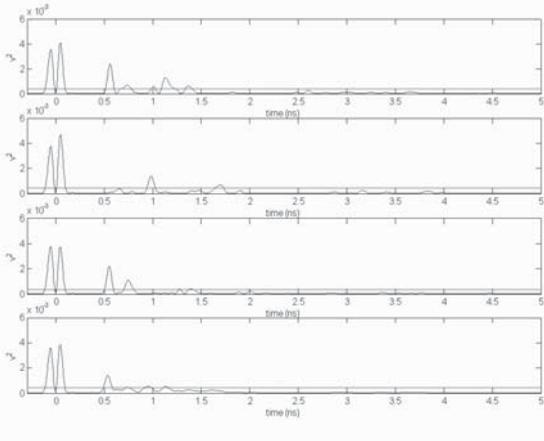
Fig. 4.   Comparison between small scale averaged power delay profiles and local power delay profiles. Measurements were performed at location W2 (TEM horn antennas, Whittemore, 2nd floor).

by averaging power along 20λ linear or circular paths independent of the signal bandwidth. An established fact is that local fading results from the destructive interference of multipath components [7]. However, for UWB signals there is no single frequency or single wavelength, thus no destructive interference can occur over the entire bandwidth of the pulse. Our observations of received signals at different points in a grid confirm the absence of small-scale fading. To quantify this effect, let us consider a signal quality defined as [33]
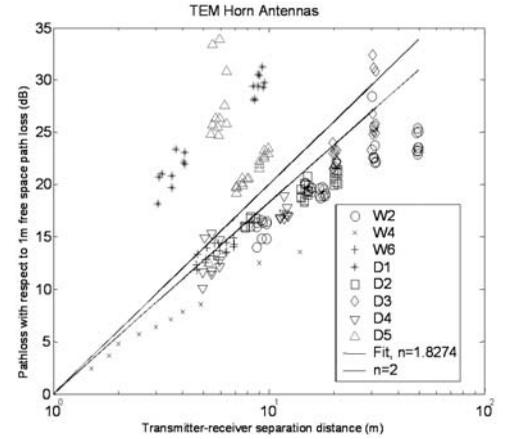
$$Q = 10 \log_{10}\left(E/E_0\right) \tag{1}$$

where E is the received signal energy given by
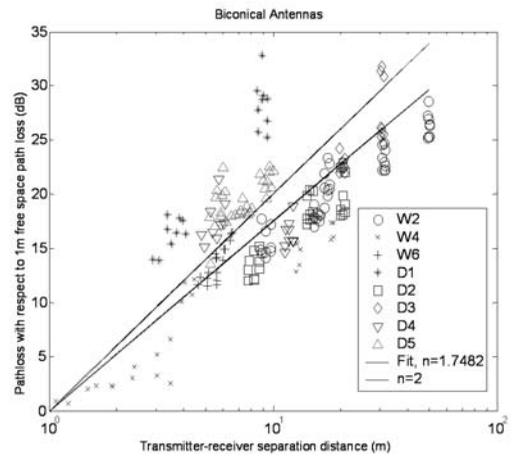
$$E = \int_0^T r^2\left(t\right) dt \tag{2}$$

with $r\left(t\right)$ being the measured multipath profile over the time duration T. Also, in (2) E_0 is the energy measured at a reference location, usually chosen to be at a 1 m distance from the transmitter. There is almost no fading as a result of interference. All local PDPs are within 3 dB of the average level unless some profiles are obstructed with some objects in the channel or they belong to points very close to walls. If transmitter and/or receiver locations are close to walls, the received profile is affected significantly [7]. Robustness of UWB communication systems, insofar as multipath is concerned, is manifested by small variations in signal quality at various grid locations [14].

B. Path-Loss and Large-Scale Analysis

The energy in the received profile decreases with the distance between the receiver and the transmitter. The path-loss exponent, n, is a measure of decay in signal power with distance, d, according to $1/d^n$. A reference measurement is performed at a distance of 1 m form the transmitter. Subsequent energy measurements are performed with respect to the reference measurement. Using the log-normal shadowing assumption, the path-loss exponent, n, is related to the

(a) For TEM horn antennas.

(b) For biconical antennas.

Fig. 5.   Scatter plots for the relative path-loss versus frequency for all locations.

received energy at distance d and the reference measurement by

$$PL\left(d\right) = \overline{PL}\left(d_0\right) + 10n \log_{10}\left(\frac{d}{d_0}\right) + X_\sigma \tag{3}$$

where d_0 is the reference distance, $\overline{PL}\left(d_0\right)$ is the average measured energy at the reference distance and X_σ is a zero-mean Gaussian distributed random variable in (dB) with standard deviation equal to σ [8]. The path-loss exponent is obtained by fitting a line on the logarithmic scatter plot of energy versus distance. The standard deviation for the Gaussian random variable is obtained by calculating the deviation from the obtained fit. The reference measurement is very important as it defines the intercept with the vertical axis and hence affects the fitted slope. Many reference measurements can be averaged together to reduce the effect of the measurement environment.

In narrowband characterization, the local PDPs and small-scale averaged PDPs (SSA-PDP) are usually used to eliminate any small-scale effect. The same technique is implemented by Cassioli et al. [11] to generate local and global parameters. In the present analysis, the UWB pulse delay time is used to find the distance between the receiver and the transmitter. First, the

Table 1. Large-scale path-loss parameters for TEM horn and biconical antennas

Antenna	TEM Horn		Biconical	
Location	n	σ	n	σ
W & D	1.8274	5.7291	1.7482	4.2585
W	1.5602	1.7196	1.5653	2.0095
W2	1.5454	1.6763	1.5807	1.3494
W4	1.2744	0.4763	1.3035	1.9032
W6	1.7845	0.7160	1.8192	1.0235
D	2.0401	6.5007	1.9103	4.8007
D1	3.2883	2.6456	2.9655	1.8769
D2	1.6591	1.0542	1.5365	1.5381
D3	1.7986	2.3358	1.7983	2.2394
D4	1.6478	1.3841	1.7870	3.9154
D5	2.6701	5.6894	2.2455	1.8009
LOS	1.6077	1.5816	1.5826	1.9135
NLOS	2.6039	6.0840	2.4118	3.2698

W: Whittemore Hall, D: Durham Hall
W2, W4, W6 : Whittemore Hall with the associated floor number
D1,D2,D3,D4,D5: Durham Hall with the associated transmitter location as in Figure 3b

distance between the transmitter and the receiver is measured at a reference position. Then, other distances separating the receiver from the transmitter are calculated using the pulse delay time. This allows us to take measurements at locations with small separation distances and reduce the error associated with distance measurements. Measured points are distributed across the entire scatter plots rather than being clustered. This distribution reduces the error associated with reference measurements. The scatter plots for global data are presented in Fig. 5.

The extracted parameters for LOS and NLOS scenarios are summarized in Table 1. The minimum pathloss exponent is 1.27 for the case of narrow corridor which has nearly the behavior of a lossy waveguide structure. The maximum pathloss exponent is 3.29 in some obstructed scenarios. The global line-of-sight parameters are n=1.61 and σ=1.58 dB for the TEM horns and n=1.58 and σ=1.91 dB for the biconical antennas. The NLOS scenarios have path-loss exponents greater than 2 and also have larger σ values compared with LOS scenarios.

In general, there is close agreement between the results obtained with directive antennas and the results obtained with omni-directional antennas. This similarity of results obtained with the two types of antennas de-emphasizes the contribution of the back reflection components. A notable difference is lower σ values when directive antennas are used, especially in

NLOS scenarios as directive antenna can be easily shadowed by any object in the channel while omni-directional antennas can still receive some components.

The reported path-loss exponents for narrowband systems are 1.6-1.8 for in-building line-of-sight environments and 4-6 for obstructed in-building environments [8]. As noted from Table 1, the path-loss exponents for UWB are comparable with path-loss exponents for narrowband LOS scenarios but are smaller for NLOS scenarios. The results for path-loss exponent and the standard deviation introduced by Ghassemzadeh et al. [19] are comparable to the results obtained from our measurements. They performed UWB frequency-domain measurements around 5 GHz [19], which is close to the center frequency in the spectrum of the pulse used in our experiments. Their parameters are n=1.7, σ=1.6 dB for LOS scenarios and n=3.5, σ=2.7 dB for NLOS scenarios.

C. Time Dispersion Results

Time dispersion parameters shed some light on the temporal distribution of power relative to the first arriving components. Delay spreads restrict transmitted data rates and could limit the capacity of the system when multi-user systems are considered. The time dispersion of UWB pulses can be presented as the ratio of the average arrival time to the spread of the
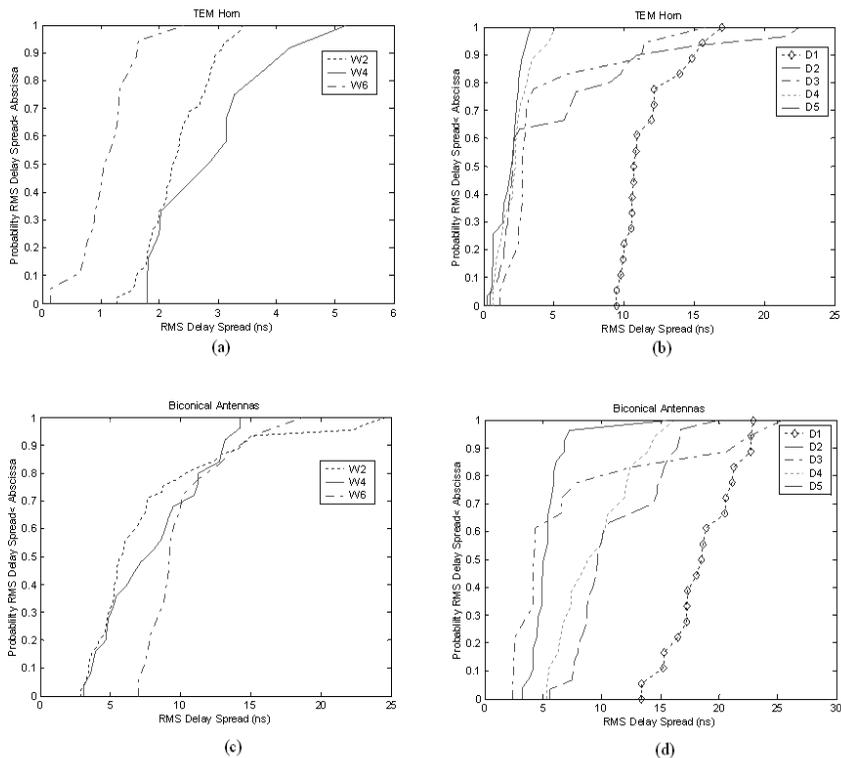
Fig. 6. Cumulative distribution functions for the RMS delay spread (20 dB): (a) Whittemore Hall using TEM horn antenna, (b) Durham Hall using TEM horn antenna, (c) Whittemore Hall using biconical antenna, (d) Durham Hall using biconical antenna.
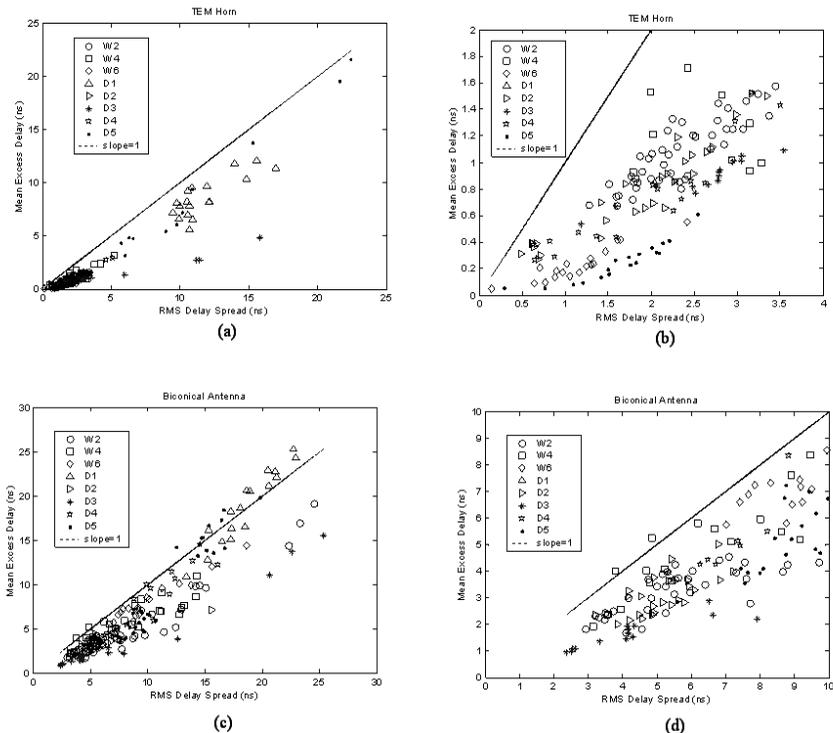

Fig. 7. Scatter plots for the mean excess delay versus the RMS delay spread: (a) TEM horn antenna, all scenarios, (b) TEM horn antenna, zoomed view, (c) biconical antenna, all scenarios, (d) biconical antenna, zoomed view.

arrival time. The formulation of time dispersion parameters is given in [8].

The ratio of the mean excess delay to the RMS delay spread can be used as a measure of the time dispersion for UWB signals. If $\sigma_\tau = \overline{\tau}$, then the multipath delay profile decays exponentially. The situation corresponds to two multipath components with equal power where the second path is $2\overline{\tau}$ away from the first component. High concentration of power when the excess delay is small is reflected by $\overline{\tau}/\sigma_\tau < 1$. When energy arrives at the mid point of the power delay profile and not at the earliest part then $\overline{\tau}/\sigma_\tau > 1$ [7].

The cumulative distribution function (CDF) for the RMS delay spread is plotted in Fig. 6. All multipath components within 20 dB of the maximum are included. Obstructed and non-line-of-sight scenarios resulted in higher time dispersion. The variations between different scenarios and buildings are less for the omnidirectional antennas than those when directive TEM horns are used. For the biconical antennas the values are higher because the receiving biconical antenna can receive more multipath components. It should be noted that the instantaneous delay spreads cannot be averaged to give the delay spread. Instead, for the SSA-PDPs, the power delay profiles are averaged and then the delay spread is calculated. Individual power delay profiles are averaged and weighted by their own power [26].

Next, the correlation between the channel time dispersion parameters is examined. The relation between the mean excess delay and the RMS delay spread is illustrated in Fig. 7. The ratio $\overline{\tau}/\sigma_\tau$ is mostly in the range of 0.25-1. The small values for this ratio imply high concentration of power at small excess delay. Obstructed measurements tend to have $\overline{\tau}/\sigma_\tau = 1$ which means that the power decays exponentially with time. For the LOS scenarios the mean excess delay is close to zero, indicating that only the LOS component is within the specified level of power. The number of dominant multipath components is limited to two in LOS scenarios. This is consistent with the results of previous measurements carried out at the same locations in Durham Hall by [30].

Scatter plots analysis of our UWB measured data indicates that there is no relationship between delay spread and transmitter-receiver (T-R) separation. This is in agreement with that reported in [7] and [1] for narrowband systems. On the other hand, when considering the relation between the received energy and the delay spread, lower energy signals might seem to have larger excess delay. However, this is because the locations where the received energy is low are usually obstructed and signals arrive at the receiver through many paths. In general, received power is not correlated to the excess delay parameters. In [7] and [1] too, scatter plots of RMS delay spread versus path-loss indicate no correlation.

IV. COMPARISON WITH UWB AND NARROWBAND PUBLISHED RESULTS

In the 5-30 m distance range, indoor channels are expected to have an RMS delay spread of 19-47 ns [34] and mean values in the range of 20-30 ns [3]. Keignart and Daniele [35] presented their measurements for a maximum distance of 10 m in an indoor UWB channel. They found that their

measured RMS delay spread varies between14 to 18 ns which is lower than that reported by Hashemi [3]. They also found that the mean excess delay increases when transmitter/receiver antenna separation increases. The mean excess delay in their experiment was 4-9 ns for LOS and 17-23 ns for NLOS scenarios.

In comparing the published results for narrowband and UWB propagation experiments, one has to consider the difference between the used pulse-shape and the associated frequency spectrum. Time dispersion parameters are functions of the noise floor. Without considering the noise power level, time dispersion parameters lose their significance. For the results presented here, unless stated otherwise, the noise floor is considered at 20 dB below the maximum instantaneous signal power.

V. CONCLUSIONS

Time-domain measurements were presented for ultra wideband indoor channel characterization. The performed measurements have the high resolution necessary for development of accurate UWB communication channel models. The high-resolution pulses used in these measurements are good candidates for small cell scenarios, such as single-cell-per-room where few obstructions exist. Directive TEM horn and omnidirectional biconical antennas were used in the measurements and their impacts on received signals were compared. Site-specific trends and general observations were also discussed. Some statistical analyses of the measured data were presented and compared with the previously published UWB and narrowband results. These measurements and the corresponding statistical analysis indicated that, unlike narrowband signals, UWB signals are immune to multipath fading. The calculated path-loss exponent was as low as 1.27 for a narrow corridor. For LOS and NLOS scenarios the global path-loss exponents were found to be nearly 1.6 and 2.7, respectively. The calculated time dispersion parameters for the measured results indicate high concentration of power at low excess time delays.

REFERENCES

[1] A. A. Saleh and R. A Valenzuela, "A statistical model for indoor multipath propagation," *IEEE J. Select. Areas Commun.*, vol. 5, no. 2, pp. 128-137, Feb. 1987.

[2] H. Hashemi, "The indoor radio propagation channel," in *Proc. IEEE*, vol. 81, no. 7, pp. 943-968, July 1993.

[3] H. Hashemi, "Impulse response modeling of indoor propagation channels," *IEEE J. Select. Areas Commun.*, vol. 11, no. 7, pp. 967-978, Sep. 1993.

[4] C. R. Anderson, T. S. Rappaport, K. Bae, A. Verstak, N. Ramakrishnan, W. Tranter, C. Shaffer, and L. Watson, "In-building wideband multipath characteristics at 2.5 & 60 GHz," in *Proc. IEEE 56th Vehicular Technology Conference*, pp. 97-101, Sep. 2002.

[5] G. D. Durgin, and T. S. Rappaport, "Theory of multipath shape factors for small-scale fading wireless channels," *IEEE Trans. Antennas Propagat.*, vol. 48, no. 5, pp. 682-693, May 2000.

[6] T. S. Rappaport and D. A. Hawbaker, "Wideband microwave propagation parameters using circular and linear polarization antennas for indoor wireless channels," *IEEE Trans. Commun.*, vol. 40, no. 2, pp. 1-6, Feb. 1992.

[7] T. S. Rappaport, "Characterization of UHF multipath radio channels in factory buildings," *IEEE Trans. Antennas Propagat.*, vol. 37, no. 8, pp. 1058-1069, Aug. 1989.

[8] T. S. Rappaport, *Wireless Communications, Principles & Practice.* Upper Saddle River, NJ: Prentice Hall, 1996.

[9] B. Uguen, E. Plouhinec, and G. Ghassay, "A deterministic ultra wideband channel modeling," in *Proc. IEEE Conference on Ultra Wideband Systems and Technologies*, pp. 1-5, May 2002.

[10] F. Zhu, Z. Wu, and C. Nassar, "Generalized fading channel model with application to UWB," in *Proc. IEEE Conference on Ultra Wideband Systems and Technologies*, pp. 13-17, May 2002.

[11] D. Cassioli, M. Win, and A. Molisch, "A statistical model for the UWB indoorchannel," in *Proc. IEEE Vehicular Technologies Conf.*, vol. 2, pp. 1159-1163, May 2001.

[12] D. Cassioli, M. Win, and A. Molisch, "The ultra-wide bandwidth indoor channel: From statistical model to simulations," *IEEE J. Select. Areas Commun.*, vol. 20, no. 6, pp. 1247-1257, Aug. 2002.

[13] S. Chalillou, D. Helal, and C. Cattaneo, "Timed simulator for UWB communication systems," in *Proc. IEEE Conference on Ultra Wideband Systems and Technologies*, pp. 6-11, May 2002.

[14] R. A. Scholtz and M. Z. Win, "Impulse radio," in *Proc. IEEE Pers. Indoor Mobile Radio Comm. Conf.*, pp. 245-267, Sep. 1997.

[15] R. Cramer, R. A. Scholtz, and M. Z. Win, "Evaluation of an ultra wideband propagation channel," *IEEE Trans. Antennas Propagat.*, vol. 50, no. 5, pp. 561-570, May 2002.

[16] H. G. Schantz and L. Fullerton, "The diamond dipole: A Gaussian impulse antenna," in *Proc. IEEE International Symposium Antenna and Propagation Society*, vol. 4, pp. 100-103, July 2001.

[17] P. Withington, R. Reinhardt, and R. Stanley, "Scanning receiver," in *Proc. IEEE Conference on Military Communications*, vol. 2, pp. 1186-1190, Oct. 1999.

[18] D. Dickson and P. Jett, "Application specific integrated circuit implementation of a multiple correlator for UWB radio applications," in *IEEE Conference*, vol. 2, pp. 1207-1210, Oct. 1999.

[19] S. Ghassemzadeh, R. Jana, C. Rice, and W. Turin, "A statistical path loss model for in-home UWB channels," in *Proc. IEEE Conference on Ultra Wideband Systems and Technologies*, pp. 59-64, May 2002.

[20] C. Prettie, D. Cheung, L. Rusch, and M. Ho, "Spatial correlation of UWB in a home environment," in *Proc. IEEE Conference on Ultra Wideband Systems and Technologies*, pp. 65-69, May 2002.

[21] J. Keignart and N. Daniele, "Subnanosecond UWB channel sounding in frequency and temporal domain," in *Proc. IEEE Conference on Ultra Wideband Systems and Technologies*, pp. 25-29, May 2002.

[22] J. Kunisch and J. Pamp, "Measurement results and modeling aspects for the UWB radio channels," in *Proc. Conference on Ultra Wideband Systems and Technologies*, pp. 19-23, May 2002.

[23] A. Street, L. Lukama, and D. Edwards, "Use of VNAs for wideband propagation measurements," in *Proc. IEE Commun.*, vol. 148, no. 6, pp. 411-415, Dec. 2001.

[24] V. Hovinen, M. Hämäläinen, and T. Pätsi, "Ultra wideband indoor radio channel models: Preliminary results," in *Proc. IEEE Conference on Ultra Wideband Systems and Technologies*, pp. 75-79, May 2002.

[25] W. A. Kissick, *The Temporal and Spectral Characteristics of Ultra Wideband Signals*, U.S. Department of Commerce, NTIA Report 01-383, Jan. 2001.

[26] R. G. Vaughan and N. Scott, "Super-resolution of pulsed multipath channels for delay spread characterization," *IEEE Trans. Commun.*, vol. 47, no. 3, pp. 343-347, Mar. 1999.

[27] R. Davies, M. Bensebti, M. A. Beach, and J. P. McGeehan, "Wireless propagation measurements in indoor multipath environments at 1.7 GHz and 60 GHz for small cell systems," in *Proc. IEEE 41st Vehicular Technology Conference*, pp. 589-593, May 1991.

[28] S. Seidel and T. Rappaport, "Site-specific propagation prediction for wireless in-building personal communication system design," *IEEE Trans. Veh. Technol.*, vol. 43, no. 4, pp. 879-891, Nov. 1994.

[29] D. A. Hawbaker, "Indoor Wideband Radio Wave Propagation Measurements and Models at 1.3 GHz and 4.0 GHz," master's thesis, Dept. Elec. Engr., Virginia Polytech. Inst. and State Univ., 1991.

[30] C. R. Anderson, "Design and Implementation of an Ultrabroadband Millimeter-Wavelength Vector Sliding Correlator Channel Sounder and In-Building Multipath Measurements at 2.5 & 60 GHz," master's thesis, Dept. Elect. & Comp. Eng., VPI & SU, 2002.

[31] R. J.-M. Cramer, M. Z. Win, and R. A. Scholtz, "Impulse radio multipath characteristics and diversity reception," *IEEE Int. Conf. on Comm.*, vol. 3, pp. 1650-1654, June 1998.

[32] G. Durgin, T. S. Rappaport, and H. Xu, "Measurements and models for radio path loss and penetration loss in and around homes and trees at 5.85 GHz," *IEEE Trans. Commun.*, vol. 46, no. 11, pp. 1484-1496, Nov. 1998.

[33] M. Z. Win, "Ultra-Wide Bandwidth Spread-Spectrum Techniques for Wireless Multiple-Access Communications," Ph.D. dissertation, University of Southern California, Electrical Engineering Department, Los Angeles, 1998.

[34] J. R. Foerster, "The effects of multipath interference on the performance of UWB systems in an indoor wireless channel," *IEEE VTS 53rd*, vol. 2, pp. 1176-1180, May 2001.

[35] J. Keignart and N. Daniele, "Subnanosecond UWB channel sounding in frequency and temporal domain," in *Proc. IEEE Conference on Ultra Wideband Systems and Technologies*, pp. 25-29, May 2002.

Ali Muqaibel was awarded the Bachelor of Science degree with highest honors from King Fahd University of Petroleum and Minerals in 1996. In 1999, he received his Master of Science degree in Electrical Engineering from KFUPM with a focus on communication systems. In 2000, Ali began work towards a Doctor of Philosophy degree in Electrical Engineering with the Time Domain and RF Measurements Laboratory (TDL). He also joined the Mobile and Portable Radio Research Group (MPRG) at Virginia Tech. In 2003, he was awarded PhD in Electrical Engineering form Virginia Polytechnic Institute and State University. While at Virginia Tech, he participated in research as well as teaching. In 2003, he joined King Fahd University of Petroleum and Minerals (KFUPM) as an assistant professor. Before that, Dr. Muqaibel had worked for three years as an electrical engineer and one year as a lecturer at KFUPM. His research interest includes: channel characterization, UWB communication, time domain and RF measurements, and channel coding. He has co-authored many technical reports and over 20 conference and journal papers.

Ahmad Safaai-Jazi received the B.Sc. degree from Sharif University of Technology, Tehran, Iran, in 1971, the M.A.Sc. degree from the University of British Columbia, Vancouver, Canada, in 1974, and the Ph.D. degree (with distinction) from McGill University, Montreal, Canada, in 1978, all in electrical engineering. From 1978 to 1984, he was an Assistant Professor with the Division of Electrical and Computer Engineering at Isfahan University of Technology. During 1984 to 1986, he was a Research Associate with the Department of Electrical Engineering at McGill University, Montreal, Canada, and carried out extensive research on acoustic wave propagation in optical fibers. In Fall 1986, Dr. Safaai-Jazi joined Virginia Polytechnic Institute and State University where he is currently a Full Professor in the Bradley Department of Electrical and Computer Engineering. His research interests include guided-wave optics, optical communications, antennas, and UWB propagation. At Virginia Tech, he introduced and developed a new graduate course, "Optical Waveguides", which is a principal graduate course in the fiber optic program. He is the author or co-author of more than 110 refereed journal papers and conference publications, has contributed two book chapters, and is the co-inventor of four patents. Dr. Safaai-Jazi received the College of Engineering Dean's Award for Teaching Excellence in 2002.

Ahmed Attiya was born on Sept. 19th 1968 in Cairo, Egypt. He received B.Sc. with honor degree in 1990 from Electrical Engineering Dept., Zagazig University, Egypt. He has worked as a research assistant in Electronics Research Institute on 1991. He received his M.Sc. and Ph.D. degrees from Electrical Engineering Dept. Cairo University, Egypt in 1996 and 2001 respectively. In 2002 he worked as a research associate in Electrical and Computer Engineering Department in Virginia Polytechnic Institute and State University. In summer of 2004, he joined the Department of Electrical Engineering at the University of Mississippi, Oxford, MS, as a visiting scholar.

His research interests include microstrip antennas, phased arrays, numerical techniques in electromagnetics, high frequency techniques, ultra wideband antennas, localized waves and propagation, scattering and diffraction of ultra wideband signals.

Brian Woerner was born on October 11, 1964. He received his B.S. degree in Computer and Electrical Engineering from Purdue University in West Lafayette, IN in 1986. He received the M.S. degree and Ph.D. degrees in Electrical Engineering Systems from the University of Michigan at Ann Arbor in 1987 and 1991, respectively. During his Ph.D. studies he was a recipient of the University of Michigan's Benton Fellowship and Unisys Fellowship. He also holds a Master of Public Policy degree from the University of Michigan's Institute of Public Policy Studies, with an emphasis in telecommunications policy. Dr. Woerner joined the faculty at Virginia Tech in Fall 1991 and held the rank of Full Professor and Associate Director of the Mobile and Portable Radio Research Group. Areas of research expertise and specialization include multiple access techniques including Code Division Multiple Access (CDMA), multiuser detection and interference cancellation, error correction techniques including turbo coding and processing, multi-antenna systems, position determination, and land mobile radio systems. Dr. Woerner received the 1999 College of Engineering Dean's Award for Teaching Excellence. He is currently Lane Professor & Chairman of the Lane Department of Computer Science and Electrical Engineering at West Virginia University.

Sedki M. Riad (M'78-SM'82-F'92) was born in Egypt, on February 19, 1946. He received the B.Sc. and M.Sc. degrees from Cairo University, Cairo, Egypt, in 1966 and 1972, respectively, both in electrical engineering, and the Ph.D. degree in engineering science from the University of Toledo, Toledo, OH, in 1976. From 1975 to 1977, he was with the National Institute for Standards and Technology (NIST), Boulder, CO, as a Guest Worker, where he was involved with post-doctoral research. In 1985, he rejoined NIST for a six-month period, while on leave from the Virginia Polytechnic Institute and State University, Blacksburg. He has held faculty positions at Cairo University (1966-73), the University of Central Florida, Orlando (1977-79), and the King Saud University, Riyadh, Saudi Arabia (1984-85). Since 1979, he has been a Professor of electrical engineering and the Director of the Time Domain and RF Measurement Laboratory at the Virginia Polytechnic Institute and State University. He has authored and co-authored one book chapter and over 100 technical journal and conferences papers. His main area of interest is microwave measurements with emphasis in time-domain techniques, instrumentation, and related device modeling, computer simulation, and signal processing. Dr. Riad is a Registered Professional Engineer in the State of Florida. He is a past chairman of the U.S. National Commission A of the International Union of Radio Science (URSI) (1994-1996). He has also been active with the IEEE Virginia Mountain Section and is past chairman of the section and has chaired several of its committees. He is an Editorial Review Board member of several IEEE societies, most particularly, the IEEE TRANSACTIONS ON INSTRUMENTATION AND MEASUREMENTS. He has served as the guest editor for an IMTC'92 Special Issue and he has participated in several of the I&M's two main conferences CPEM and IMTC.